

Towards Accurate Post-Training Quantization for Vision Transformer

Yifu Ding^{1,2,3}, Haotong Qin^{1,3}, Qinghua Yan¹,
Zhenhua Chai², Junjie Liu², Xiaolin Wei², Xianglong Liu^{†,1}
¹ State Key Laboratory of Software Development Environment, Beihang University
² Meituan ³ Shen Yuan Honors College, Beihang University
{yifuding, haotongqin, yanqh, xliu}@buaa.edu.cn, {chaizhenhua, liujunjie10, weixiaolin02}@meituan.com

ABSTRACT

Vision transformer emerges as a potential architecture for vision tasks. However, the intense computation and non-negligible delay hinder its application in the real world. As a widespread model compression technique, existing post-training quantization methods still cause severe performance drops. We find the main reasons lie in (1) the existing calibration metric is inaccurate in measuring the quantization influence for extremely low-bit representation, and (2) the existing quantization paradigm is unfriendly to the power-law distribution of Softmax. Based on these observations, we propose a novel Accurate Post-training Quantization framework for Vision Transformer, namely APQ-ViT. We first present a unified *Bottom-elimination Blockwise Calibration* scheme to optimize the calibration metric to perceive the overall quantization disturbance in a blockwise manner and prioritize the crucial quantization errors that influence more on the final output. Then, we design a *Matthew-effect Preserving Quantization* for Softmax to maintain the power-law character and keep the function of the attention mechanism. Comprehensive experiments on large-scale classification and detection datasets demonstrate that our APQ-ViT surpasses the existing post-training quantization methods by convincing margins, especially in lower bit-width settings (e.g., averagely up to 5.17% improvement for classification and 24.43% for detection on W4A4). We also highlight that APQ-ViT enjoys versatility and works well on diverse transformer variants.

CCS CONCEPTS

• Computing methodologies → Computer vision problems.

KEYWORDS

post-training quantization, vision transformer, computer vision

ACM Reference Format:

Yifu Ding^{1,2,3}, Haotong Qin^{1,3}, Qinghua Yan¹, Zhenhua Chai², Junjie Liu², Xiaolin Wei², Xianglong Liu^{†,1}. 2022. Towards Accurate Post-Training Quantization for Vision Transformer. In *Proceedings of the 30th ACM International*

[†]Corresponding author.

Permission to make digital or hard copies of all or part of this work for personal or classroom use is granted without fee provided that copies are not made or distributed for profit or commercial advantage and that copies bear this notice and the full citation on the first page. Copyrights for components of this work owned by others than ACM must be honored. Abstracting with credit is permitted. To copy otherwise, or republish, to post on servers or to redistribute to lists, requires prior specific permission and/or a fee. Request permissions from permissions@acm.org.

MM '22, October 10–14, 2022, Lisboa, Portugal

© 2022 Association for Computing Machinery.

ACM ISBN 978-1-4503-9203-7/22/10...\$15.00

<https://doi.org/10.1145/3503161.3547826>

Conference on Multimedia (MM '22), October 10–14, 2022, Lisboa, Portugal.
ACM, New York, NY, USA, 9 pages. <https://doi.org/10.1145/3503161.3547826>

1 INTRODUCTION

With the development of deep learning, the neural networks achieve great success in a various domains, such as image classification [24, 37, 39, 42–44], object detection [13, 14, 26, 33, 36, 45], semantic segmentation [11, 51], etc. Recently, the Vision Transformer (ViT) [9] emerges as a novel and effective architecture and shows great potential for various vision tasks. However, pretrained models usually have massive parameters and considerable computational overheads, e.g., the ViT-L model is with 307M parameters and 190.7 GFLOPs during inference [9]. The high computational complexity and non-negligible latency hinder the practical applications of vision transformers in real-world applications especially on edge devices. To address the challenge, many architectures have been proposed for lightweight vision transformers ([32], [15], [31]). Although these works have achieved remarkable speedup and memory footprint reduction, they still rely on floating-point operations, leaving room for further compression by parameter quantization.

As a model compression approach, quantization compacts the floating-point parameters of neural networks to lower-bit representations, and the computation can be implemented by efficient integer operations on hardware. Thus, quantized vision transformers significantly save the storage and speed up inference. Considering that re-training the transformer is time-consuming and computationally intensive, Post-Training Quantization (PTQ) is a practical solution in widespread scenarios, which just takes a small unlabeled dataset to quantize (calibrate) a pre-trained network with no need for training or fine-tuning. Many previous works are devoted to quantizing vision transformers [28, 30, 47], which shows great potential in both accuracy and efficiency. Applying the existing methods can almost retain the original accuracy of full-precision transformers under the 8-bit setting.

However, when quantizing the vision transformer to ultra-low bit-widths (e.g., 4-bit weight and activation), the model suffers severe accuracy drop or even crashes. Our study reveals that the poor performance might attribute to two issues from optimization and structure perspectives. From the optimization perspective, the limited bit-width constraints the representation capability and causes larger errors which makes the existing second-order layerwise calibration metric not accurate in measuring the impact of quantization error on the final output. And as for the structure perspective, the existing quantization paradigm is unfriendly to the Softmax function in the attention mechanism, which is also known as a normalized exponential function. It redistributes the inputs to

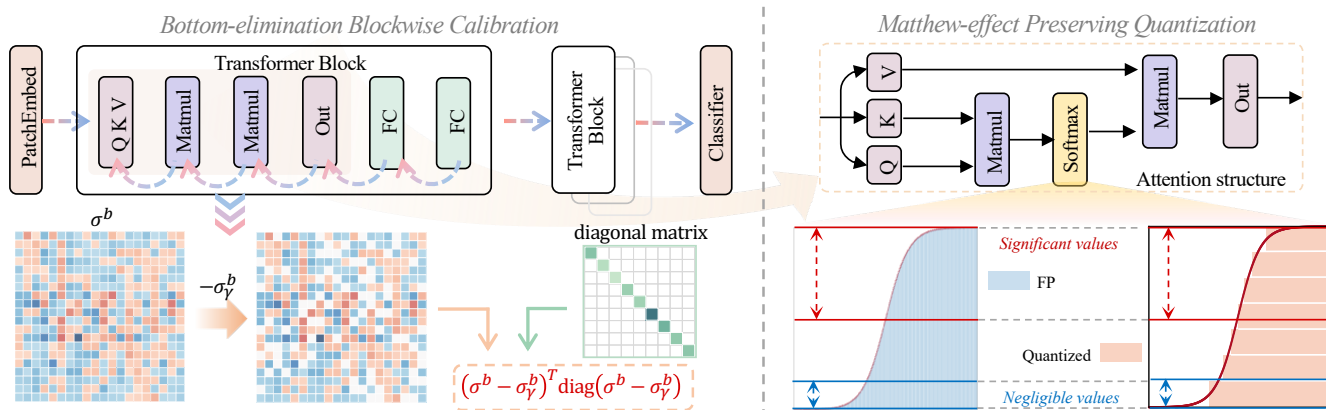


Figure 1: Overview of APQ-ViT. The left is **Bottom-elimination Blockwise Calibration** to apply quantization in a blockwise manner to perceive the quantization loss of adjacent layers, and prioritize the significant errors by eliminating the second-order gradient corresponding to trivial errors. The right is **Matthew-effect Preserving Quantization**, which is specialized for maintaining the power-law distribution of the Softmax function.

satisfy the power-law probability, while we discover that previous quantization solutions are easy to damage the Matthew-effect of Softmax. Therefore, specializing in the quantization strategy for vision transformers is a great need to improve the accuracy of the low-bit quantized model.

In this paper, we propose an accurate post-training quantization method for vision transformers, namely APQ-ViT, which considers both the optimization difficulty and the special structure for low bit-width (See the overview in Figure 1). First, we present a unified *Blockwise Bottom-elimination Calibration* (BBC) scheme to optimize the calibration metric based on the block-stacking architecture, which can be flexibly generalized to other variants. It enables the metric to perceive the quantization loss in a blockwise manner and prioritize the significant errors by eliding the second-order gradients corresponding to the inevitable trivial errors. Second, the *Matthew-effect Preserving Quantization* (MPQ) is specifically tailored for the Softmax function. Instead of obeying the maximizing mutual information paradigm as many quantization methods, we hold the view that preserving the power-law distribution in the quantized Softmax is more crucial for the attention mechanism.

Our APQ-ViT revisits the process of post-training quantization for vision transformer and presents novel insights. Comprehensive experiments on the large-scale computer vision tasks (image classification [7] and object detection [27]) demonstrate that our APQ-ViT performs remarkably well across various transformer architectures such as ViT [9], DeiT [41], and Swin Transformer [29], and surpasses the existing methods by convincing margins, especially in lower bit-width settings (e.g., averagely up to 5.17% improvement for classification and 24.43% for detection on W4A4). We highlight that our APQ-ViT scheme achieves state-of-the-art accuracy performance on various bit-width settings, and enjoys versatility on diverse architectures and vision tasks.

We summarize our main contributions as:

- We find that for the post-training quantization of vision transformer, (1) the extremely low-bit representation makes the existing calibration metric inaccurate in measuring the quantization

errors; and (2) an inconsistency exists between the quantization paradigm and the power-law distribution of Softmax.

- We present an accurate post-training quantization method for vision transformer, namely APQ-ViT, with a unified Blockwise Bottom-elimination Calibration scheme to enable the quantization perception inside blocks and prioritize the crucial errors that influence the final predictions.
- Our study reveals the power-law distribution of the Softmax function and proposes the Matthew-effect Preserving Quantization. In contrast to purely minimizing the quantization loss, it inspires a novel perspective to preserve the character of Softmax while embedding quantization.
- We evaluate the APQ-ViT on large-scale image classification and object detection tasks with different model variants and bit-width, and obtain prevailing improvements over existing post-training quantization methods especially in lower bit-width.

2 RELATED WORK

2.1 Vision Transformer

The classical vision transformer [9] is constructed by pure transformer targeting to process image patches, which is stacked by several attention-based blocks that are composed of a multi-head self-attention module and multi-layer perceptron. DETR [4] further extends to object detection, which uses ResNet as the backbone and replaces the detection head with transformers. Following them, there are many variants for more applications with new techniques specialized for CV applications [10, 25, 34, 35]. Swin Transformer [29] emerges as a competitive backbone with excellent generalization capability for many benchmarks and remarkably surpasses the state-of-the-art CNNs in most CV tasks.

Many works are also devoted to balancing performance and efficiency. MobileViT exploits global representation capability and spatial order preservation of transformer by inserting it into convolution blocks. Some works simplify the attention mechanism, like sparse attention [3, 48], linear approximate attention [5, 21]

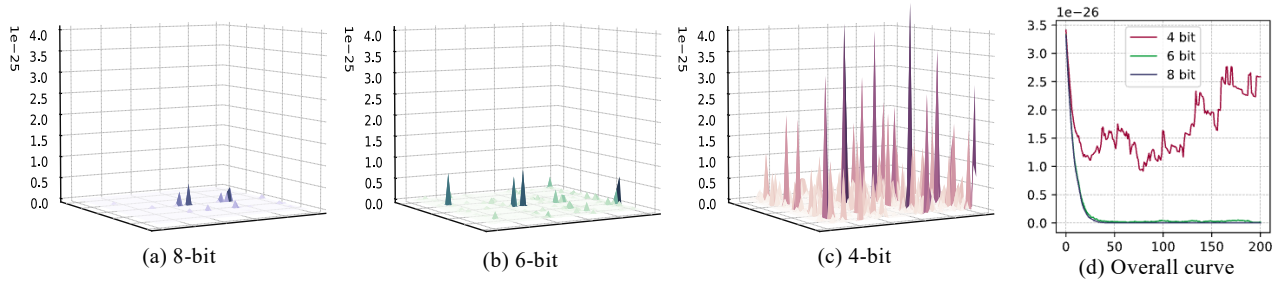


Figure 2: Visualization of Hessian-guided loss term of the optimal scaling factor for (a) 8-bit, (b) 6-bit and (c) 4-bit quantization. And (d) shows the curve of overall loss terms for all the candidates.

QuadTree attention [40], or hashing-based attention [23]. Moreover, general model compression techniques are also actively applied. DeiT introduces distillation tokens to better interact with the teacher model through attention. [50] prunes vision transformers by sparsifying the unnecessary feature channels by ranking the importance. [16] combines NAS and parameter sharing to search and replace some self-attention modules by convolutions to improve the locality extraction. The above methods focus on optimizing the transformer architectures while keep the parameters full-precision, leaving room for further compression by quantization.

2.2 Quantization

Model quantization is one of the promising compression approaches, which quantizes the full-precision parameters to lower bit-width. It can not only shrink the model size but reduce computational complexity by transforming floating-point calculations to fixed-point, which significantly accelerates the inference, decreases the memory footprint, and reduces energy consumption. Current quantization methods can be categorized as Quantization-aware Training (QAT) and Post-training Quantization (PTQ) according to whether training/fine-tuning or not. Considering that training vision transformers is computationally intensive and time-consuming, they always have a huge demand for computation and power resources that emits lots of carbon footprint. PTQ, a training-free method, is well recognized as a more feasible solution, which can be broadly divided into two types: 1) searching best scale factor. 2) optimizing calibration strategy. To search best scale factors, [6] proposes an optimal MSE to select the scale factor that minimizes the quantization error. [47] uses Twin Uniform Quantization that specially designs two scales for long-tail parameter distribution of Softmax and GeLU, and proposes Hessian Guided Metric to search for best scales. [12] also use Piecewise Linear Quantization to make the quantized parameters better fit the bell-shaped distribution of weight and activation after scaling. As for the calibration strategy, AdaQuant [17, 19] utilizes layerwise optimization, which fixes the error induced by quantizing former layers by sequential calibration. EasyQuant [8] uses an alternative scale optimization of weight and activation, fixing one and optimizing the other throughout the network. [2] minimizes the quantization error by module-wise reconstruction to jointly optimize all the coupled linear layers inside each module.

3 METHOD

In this section, we propose an accurate post-training quantization framework for vision transformer, namely APQ-ViT. We first present the basic quantization pipeline and then introduce our techniques, including *Blockwise Bottom-elimination Calibration* (BBC) to tackle the optimization difficulties in low bit-width and the *Matthew-effect Preserving Quantization* (MPQ) to preserve the power-law redistribution for Softmax function.

3.1 Preliminaries

As a widespread solution, the asymmetric uniform quantization is applied to quantize network. And in a standard quantization transformer, the input data first passes through a quantized embedding layer before being fed into the quantized transformer blocks, and each transformer block consists of an MSA module and an MLP. The computation of MSA depends on queries \mathbf{Q} , keys \mathbf{K} and values \mathbf{V} , which are derived from hidden states \mathbf{H} . In a specific quantized transformer layer, \mathbf{H} is first quantized to $\hat{\mathbf{H}}$ before passing through linear layers, which can be expressed as

$$\hat{\mathbf{Q}} = \hat{\mathbf{w}}_Q \hat{\mathbf{H}}, \hat{\mathbf{K}} = \hat{\mathbf{w}}_K \hat{\mathbf{H}}, \hat{\mathbf{V}} = \hat{\mathbf{w}}_V \hat{\mathbf{H}}, \quad (1)$$

where $\hat{\mathbf{w}}_Q$, $\hat{\mathbf{w}}_K$, $\hat{\mathbf{w}}_V$ represent quantized weight of three different linear layers for \mathbf{Q} , \mathbf{K} , \mathbf{V} respectively. The computation of self-attention is formulated as Eq. (2):

$$\text{Attention}_q(\mathbf{Q}, \mathbf{K}, \mathbf{V}) = \text{softmax}_q \left(\frac{\hat{\mathbf{Q}} \times \hat{\mathbf{K}}^T}{\sqrt{d}} \right) \times \hat{\mathbf{V}}, \quad (2)$$

where d is the hidden size of the head and softmax_q denotes the Softmax function with quantized output. The outputs of multiple heads are concatenated together as the output of MSA. Moreover, the MLP contains two quantized linear layers, and the GeLU activation function is used after the first layer.

Among the existing post-training quantization methods for vision transformers, one of the representatives is PTQ4ViT [47], which is a typical representation of these works using the Hessian guided metric to determine the scaling factors. In classification task, the task loss is $\mathcal{L} = \text{CE}(\hat{y}, y)$, where CE is cross-entropy, \hat{y} is the output of the network and y is the ground truth. The expectation of loss is a function of network parameters \mathbf{x} , which is $\mathbb{E}[\mathcal{L}(\mathbf{x})]$. The quantization brings a small perturbation ϵ on parameter $\hat{\mathbf{x}} = \mathbf{x} + \epsilon$. We analyze the influence of quantization to the task

loss by Taylor series expansion:

$$\mathbb{E}[\mathcal{L}(\hat{\mathbf{x}})] - \mathbb{E}[\mathcal{L}(\mathbf{x})] \approx \epsilon^T \bar{\mathbf{g}}^{(\mathbf{x})} + \frac{1}{2} \epsilon^T \bar{\mathbf{H}}^{(\mathbf{x})} \epsilon, \quad (3)$$

where $\bar{\mathbf{g}}^{(\mathbf{x})}$ is the gradients and $\bar{\mathbf{H}}^{(\mathbf{x})}$ is the Hessian matrix. The target is to find the scaling factors to minimize the influence: $\min_{\Delta} (\mathbb{E}[\mathcal{L}(\hat{\mathbf{x}})] - \mathbb{E}[\mathcal{L}(\mathbf{x})])$. Since weight's perturbation ϵ is relatively small, we have a first-order Taylor expansion that $(\hat{O} - O) \approx \mathbf{g}_O(\mathbf{x})\epsilon$, where $\hat{O} = (\hat{\mathbf{x}} + \epsilon)^T \hat{\mathbf{x}}$. The second-order term in Eq. (3) could be written as

$$\epsilon^T \bar{\mathbf{H}}^{(\mathbf{x})} \epsilon \approx (\hat{O} - O)^T \bar{\mathbf{H}}^{(O)} (\hat{O} - O). \quad (4)$$

Then we follow [8, 47] to traverse the search spaces of $\Delta_{\mathbf{x}}$ by linearly dividing $\left[\alpha \frac{x_{\max} - x_{\min}}{2^k}, \beta \frac{x_{\max} - x_{\min}}{2^k} \right]$ to n candidates. α and β are two parameters to control the search range. We alternatively search for the optimal scaling factors $\Delta_{\mathbf{w}}^*$ and $\Delta_{\mathbf{a}}^*$ in the search space. Firstly, $\Delta_{\mathbf{a}}$ is fixed, and we search for the optimal $\Delta_{\mathbf{w}}$ to minimize loss \mathcal{L} . Secondly, $\Delta_{\mathbf{w}}$ is fixed, and we search for the optimal $\Delta_{\mathbf{a}}$ to minimize \mathcal{L} . $\Delta_{\mathbf{w}}$ and $\Delta_{\mathbf{a}}$ are alternately optimized for several rounds.

3.2 Blockwise Bottom-elimination Calibration

From the optimization perspective, existing typical post-training quantization methods for vision transformers use the second-order Hessian-guided metric to measure the quantization loss caused by each candidate scaling factor and then determine the optimal quantizer. However, we find that for the extremely low-bit representation, the layerwise optimization is inaccurate since it is unable to perceive the quantization in a higher block scale, and the quantization error is inevitably larger while the dense Hessian matrix loses the attention of the significant errors.

Ideally, we expect to determine the quantizer with the smallest quantization loss by a carefully designed loss term, and the loss should be significantly smaller compared to other candidates which converges to a local optimum. But in practice, we find that the Hessian-guided loss terms calculated by each candidate have large variance, especially at ultra-low bits (such as 4-bit). As shown in Figure 2, when we quantize the model to 8-bit, the quantization loss is steady and relatively small, the optimal loss plane in Figure 2(a) is also flat. However, when the bit-width is reduced to 4-bit, the behavior of adjacent candidates shows a significant difference, and the loss curve fluctuations heavily. Even the optimal candidate has lots of spikes on the loss plane (see Figure 2(c)). The phenomena reveal the defects of the current calibration strategy, due to the higher degree of discretization in lower-bit quantization, (1) the loss in a single layer is larger, which has an impact on the calibration of other layers in the layerwise calibration strategy, (2) the quantization loss of each element varies greatly that times larger than 8-/6-bit quantization.

Therefore, we propose a **Blockwise Bottom-elimination Calibration** (BBC) scheme for the post-training quantization. It optimizes the calibration in a blockwise manner which enables the Hessian-guided loss to have a perception of the quantization error of adjacent layers in a single block. And It uses the bottom-elimination mechanism to focus on the critical errors that influence the final output instead of the whole loss plane.

Firstly, we built a blockwise calibration scheme from post-training quantization. Taking b -th block with L layers as an example, the

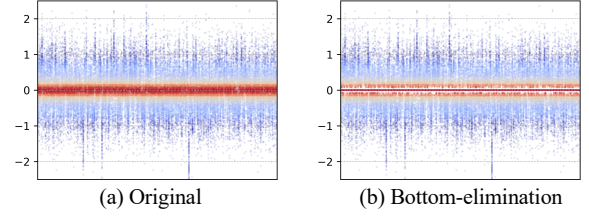


Figure 3: The quantization error measured by Hessian-based metric. Y-axis represents the magnitude of errors. (a) is the whole error distribution, and (b) visualizes the elimination of error in the 10th percentile.

computation in the block can be represented as

$$O^b = \mathbf{w}_L^{bT} \mathbf{w}_{L-1}^b \dots \mathbf{w}_1^{bT} \mathbf{a}^b, \quad (5)$$

where \mathbf{a}^b and O^b denote the input and output of the b -th transformer block. When the l -th layer is calibrated, the L -th to l -th layers can be considered as a composite layer, and its weight and activation is expressed as

$$\mathcal{W}_l^b = \mathbf{w}_L^{bT} \dots \mathbf{w}_{l+1}^b \mathbf{w}_l^{bT}, \quad \mathcal{A}_l^b = \mathbf{w}_{l-1}^b \dots \mathbf{w}_1^{bT} \mathbf{a}^b, \quad (6)$$

Taking the weight calibration as an example, the second-order term of the l -th layer in b -th transformer block can be expressed as

$$\begin{aligned} \epsilon_l^{bT} \bar{\mathbf{H}}^{(\mathcal{W})} \epsilon_l^b &= \left(J_{O^b}(\mathcal{W}_l^b) \epsilon_l^b \right)^T \bar{\mathbf{H}}^{(O^b)} J_{O^b}(\mathcal{W}_l^b) \epsilon_l^b \\ &\approx \mathbb{E} \left[\sigma^{bT} \text{diag} \left(\left(\frac{\partial \mathcal{L}}{\partial O_1^b} \right)^2, \dots, \left(\frac{\partial \mathcal{L}}{\partial O_{|O^b|}^b} \right)^2 \right) \sigma^b \right], \end{aligned} \quad (7)$$

where $\epsilon_l^b = \mathcal{W}_l^b - \hat{\mathcal{W}}_l^b$, $\sigma^b = \hat{O}^b - O^b$, and O^b , \hat{O}^b are the outputs of the b -th block before and after quantization, respectively. O_i^b denotes the i -th dimension of O^b , where $i \in [1, |O^b|]$. Therefore, we optimize the calibration metric to enable the perception of the whole block and reduce the impact on the final output.

Secondly, since the quantization error is deemed as inevitable in rounding operation and significantly increases when the bit-width is smaller, the larger errors should be of major concern. Inspired by [1, 38, 46, 49] that pruning the gradients close to zero in the backward propagation has a tiny impact on weight-updating. To pay more attention to the large errors that perturb the final output and also strike a balance between the range and variance of error, we further propose the bottom-elimination mechanism to obtain a sparse Hessian matrix in the optimization scheme. It considers the Hessian-based metric as weighted second-order gradients, and prunes the gradients that correspond to the smallest absolute quantization errors. Specifically, we construct a bottom-elimination matrix σ_γ^b for the $\sigma^b = \hat{O}^b - O^b$, which aims to select the elements with absolute values in γ -th percentile:

$$\sigma_\gamma^b = \sigma^b [\sigma^b]_\gamma, \quad [\sigma^b]_\gamma = \begin{cases} 1, & \text{where } \sigma^b < |\sigma^b|_\gamma, \\ 0, & \text{otherwise,} \end{cases} \quad (8)$$

where $[\cdot]$ denotes the *Iverson bracket* [18]. We apply the bottom elimination matrix σ_γ^b to Eq. (7) so that the obtained metric reflects

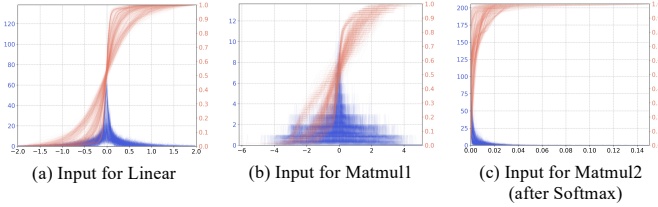


Figure 4: Visualization of different input activation distribution in the pretrained vision transformer model. (c) presents an extreme unbalanced distribution.

the critical elements in quantization that causes larger quantization error, and the optimization objective function is expressed as:

$$\min_{\Delta} \mathbb{E} \left[\left(\sigma^b - \sigma_y^b \right)^T \text{diag} \left(\left(\frac{\partial \mathcal{L}}{\partial O_1^b} \right)^2, \dots, \left(\frac{\partial \mathcal{L}}{\partial O_{|O^b|}^b} \right)^2 \right) \left(\sigma^b - \sigma_y^b \right) \right]. \quad (9)$$

Figure 3 visualizes the effect of the bottom-elimination mechanism for quantization errors. With the matrix σ_y , we optimize the calibration metric to make it focuses on perturbations with large magnitude which have nonnegligible influence on the final output of task predictions.

3.3 Matthew-effect Preserving Quantization

The special architecture of the attention mechanism in the vision transformer is also an obstacle to low-bit quantization. Especially the Softmax function, also known as the normalized exponential function, is well recognized to be unfriendly to quantization. Generally speaking, as shown in Section 3.1, each block in the vision transformer usually contains three types of computation: Linear operation, Matmul operation, and Softmax operation, these three operations involve the majority of quantized representations. We show a typical distribution of the activation inputs in Figure 4. We can see that the input distributions of the Linear and Matmul1 are similar to the Gaussian and Laplacian distributions that common methods can well quantize. However, the output of the Softmax operation obeys the power-law probability distribution, which is asymmetric and extremely unbalanced.

As a consensus, the ideal quantized parameters should retain the information of full-precision counterparts as much as possible, which is formulated as:

$$\arg \max_{\mathbf{x}, \hat{\mathbf{x}}} \mathcal{I}(\mathbf{x}; \hat{\mathbf{x}}) = \mathcal{H}(\mathbf{x}) - \mathcal{H}(\hat{\mathbf{x}} | \mathbf{x}), \quad (10)$$

where $\mathcal{H}(\hat{\mathbf{x}})$ is the information entropy, and $\mathcal{H}(\hat{\mathbf{x}} | \mathbf{x})$ is the conditional entropy of $\hat{\mathbf{x}}$ given \mathbf{x} . Since we use the deterministic quantization function, the value of $\hat{\mathbf{x}}$ fully depends on the value of \mathbf{x} , *i.e.*, $\mathcal{H}(\hat{\mathbf{x}} | \mathbf{x}) = 0$. Thus, the objective function is equivalent to maximizing the information entropy:

$$\arg \max_{\hat{\mathbf{x}}} \mathcal{H}(\hat{\mathbf{x}}) = - \sum_{\hat{x} \in \hat{\mathcal{X}}} p_{\hat{x}}(\hat{x}) \log p_{\hat{x}}(\hat{x}), \quad (11)$$

where $p_{\hat{x}}$ denotes the probability mass function of quantized parameter $\hat{\mathbf{x}}$. The formulation suggests that a well-optimized quantizer tends to make the probabilities in each quantization interval equal.

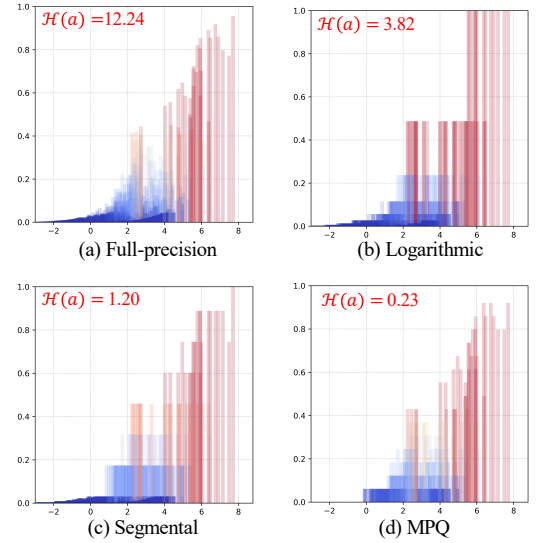


Figure 5: Comparison of quantizing attention scores with different quantizers under 4-bit setting. The x-axis is the attention values before softmax, and the y-axis is (a) full-precision or quantized to 4-bit using (b) Logarithmic quantizer, (c) Segmental quantizer [47] and (d) MPQ quantizer. The left-top values are mutual information of each distribution.

Interestingly, we observe that the quantization behavior of the Softmax function breaks the widespread idea in a counter-intuitive way. Softmax is often used as an activation function to stable the network since it can control the largest value computed in each exponent, which can be written as:

$$\text{softmax}(\mathbf{x})_i = \frac{e^{\beta x_i}}{\sum_{j=1}^K e^{\beta x_j}}, \text{ for } i = 1, \dots, K, \quad (12)$$

where $\beta \in \mathbb{R}$, and usually $\beta = 1$ in neural networks. It creates extreme asymmetric and unbalanced distributions by converting to the exponent. Therefore, many methods are devoted to designing specific quantizers for the quantization of Softmax output to maximize the information, such as Segmental quantizers [12, 47], Logarithmic quantizers [22, 28] or apply sparsification before quantization [20]. As shown in Figure 5, the Logarithmic quantizer has the largest 3.82 mutual information. It utilizes up to 11 intervals (about 69%) to represent the values clustered in $[0, 0.01]$ (about 89%), while only spares 5 fixed-points to map the rest range $(0.01, 1]$. And Segmental quantizer also utilizes more bits to cover the small values.

However, consider the original function of Softmax, when $\beta > 0$, the function will create probability distributions that are more concentrated around the positions of the largest input values. To put it simply, Softmax makes the small values even smaller while the larger values take the most probability, which is a typical phenomenon of the Matthew-effect. This character helps neural networks to stable the activation flow. Transformer architecture also adopts the Softmax as activation functions to compute the attention scores which measures the relationship of one patch in the sequence with

all the other patches. Unfortunately, existing quantizers prioritize the overall mutual information while ignoring the Matthew-effect of the Softmax function. For the significant large values, the Logarithmic and Segmental quantizers only spare fewer bits, thus the information in the larger values is damaged.

Therefore we present a **Matthew-effect Preserving Quantization (MPQ)** to quantize the Softmax output. It does not purely pursue the maximization of mutual information before and after quantization, but maintains the Matthew-effect of Softmax output during the quantization process. A typical MPQ is an asymmetric linear quantization, which can be expressed as:

$$\hat{x}_s = \text{clamp} \left(\left\lfloor \frac{\text{softmax}(\mathbf{x})}{\Delta} \right\rfloor, 0, 2^k - 1 \right), \quad \Delta = \frac{\max(\text{softmax}(\mathbf{x}))}{2^k - 1}. \quad (13)$$

where Δ is the scaling factor, and $\lfloor \cdot \rfloor$ means rounding operation. MPQ is a straightforward method that brings no extra implementation and inference overhead, and we find that it significantly improves the performance compared with other quantizers. As shown in Figure 5, MPQ allocates more bits to the larger range, where the values are sparse but significant. In this way, the important values are quantized with finer representations, which better preserves the function of Softmax.

Algorithm 1 The optimization pipeline of APQ-ViT

Input: Pre-trained vision transformer model and calibration set;

Output: Optimal scaling factors Δ^* for all layers;

```

1: for  $b = 1 : \#Block$  do
2:   Forward propagation to get full-precision  $O^b$  with the computation process  $AB$  in each layer and get loss  $\mathcal{L}$ ;
3: end for
4: for  $b = 1 : \#Block$  do
5:   Backward propagation to get  $\frac{\partial \mathcal{L}}{\partial O^b}$ ;
6: end for
7: for  $b = 1 : \#Block$  do
8:   for  $l = \#Layer : 1$  do
9:     initialize scaling factor  $\Delta_{B_l^b}^* \leftarrow \frac{B_{l_{max}}^b - B_{l_{min}}^b}{2^k}$  for  $B_l^b$ ;
10:    for search_round= 1 :  $\#Round$  do
11:      searching scaling factor  $\Delta_{A_l^b}^*$  for  $A_l^b$  using Eq. (9);
12:      searching scaling factor  $\Delta_{B_l^b}^*$  for  $B_l^b$  using Eq. (9);
13:    end for
14:  end for
15: end for
16: return Optimal scaling factors  $\Delta^*$ .

```

3.4 Framework of APQ-ViT

We propose an Accurate Post-training Quantization framework for vision transformer, namely APQ-ViT. The quantization process is shown as Algorithm 1. The APQ-ViT mainly depends on two novel techniques: BBC aims to improve the second-order calibration metric and MPQ specializes in the Softmax structure. In the calibration process, APQ-ViT first obtains the output and gradient of each transformer block through a forward and backward

Table 1: Ablation study of BBC and MPQ.

| #bit(W/A) | BBC | MPQ | ViT-S | ViT-B | DeiT-B |
|----------------|-----|-----|--------------|--------------|--------------|
| Full-precision | | | 81.39 | 84.54 | 81.80 |
| 4/4 | ✓ | | 42.57 | 30.69 | 64.39 |
| | | ✓ | 42.86 | 38.40 | 65.57 |
| | ✓ | ✓ | 46.16 | 35.44 | 66.98 |
| | | | 47.95 | 41.41 | 67.48 |
| 6/6 | ✓ | | 78.63 | 81.65 | 80.25 |
| | | ✓ | 78.78 | 81.84 | 80.33 |
| | ✓ | ✓ | 78.95 | 82.20 | 80.38 |
| | | | 79.10 | 82.21 | 80.42 |
| 8/8 | ✓ | | 81.00 | 84.09 | 81.48 |
| | | ✓ | 81.01 | 84.18 | 81.63 |
| | ✓ | ✓ | 81.15 | 84.23 | 81.68 |
| | | | 81.25 | 84.26 | 81.72 |

Table 2: Results of different post Softmax quantizers.

| #bit(W/A) | Quantizer | ViT-S | DeiT-S | DeiT-B |
|----------------|-----------|--------------|--------------|--------------|
| Full-precision | - | 81.39 | 79.85 | 81.80 |
| 4/4 | Log | 44.72 | 21.59 | 60.91 |
| | Segmental | 37.70 | 22.31 | 60.02 |
| | MPQ | 47.95 | 43.55 | 67.48 |
| 6/6 | Log | 78.94 | 77.57 | 80.34 |
| | Segmental | 78.67 | 76.64 | 80.37 |
| | MPQ | 79.10 | 77.76 | 80.42 |
| 8/8 | Log | 81.13 | 79.76 | 81.70 |
| | Segmental | 81.00 | 79.47 | 81.70 |
| | MPQ | 81.25 | 79.78 | 81.72 |

propagation and then optimizes all transformer layers in a block-wise manner with a bottom-elimination second-order metric. And MPQ is straightforwardly embedded as a quantizer after Softmax function in the Matmul operation.

As for computation intensity, compared with existing methods, the execution process of APQ-ViT only needs to store the output and gradient of each transformer block instead of all the layers, which greatly reduces the storage footprint required for the entire process (reduced to about 20%). It allows the process to be performed entirely in GPU memory to reduce the speed penalty caused by the data exchange with storage.

4 EXPERIMENT

In this section, we first demonstrate the fundamental pipeline of post-training quantization and the experimental settings. We start by ablation studies to evaluate the effectiveness of each proposed approach. And then We compare with other methods on both image classification and detection tasks with various vision transformer architectures.

Table 3: Comparison of different post-training quantization methods on image classification task with various vision transformer architectures and bit-widths.

| Method | #bit(W/A) | ViT-T | ViT-S | ViT-S/32 | ViT-B | DeiT-T | DeiT-S | DeiT-B | Swin-S | Swin-B | Swin-B/384 |
|----------------|-----------|--------------|--------------|--------------|--------------|--------------|--------------|--------------|--------------|--------------|--------------|
| Full-precision | 32/32 | 75.47 | 81.39 | 75.99 | 84.54 | 72.21 | 79.85 | 81.80 | 83.23 | 85.27 | 86.44 |
| FQ-ViT | 4/4 | 0.10 | 0.10 | 0.10 | 0.10 | 0.10 | 0.10 | 0.10 | 0.10 | 0.10 | 0.10 |
| PTQ4ViT | 4/4 | 17.45 | 42.57 | 35.09 | 30.69 | 36.96 | 34.08 | 64.39 | 76.09 | 74.02 | 78.84 |
| APQ-ViT (Ours) | 4/4 | 17.56 | 47.95 | 41.53 | 41.41 | 47.94 | 43.55 | 67.48 | 77.15 | 76.48 | 80.84 |
| FQ-ViT | 8/4 | 0.10 | 0.10 | 0.10 | 0.10 | 0.10 | 0.10 | 0.10 | 0.10 | 0.10 | 0.10 |
| PTQ4ViT | 8/4 | 36.17 | 63.00 | 49.68 | 71.64 | 48.00 | 36.08 | 70.07 | 80.13 | 81.45 | 83.75 |
| APQ-ViT (Ours) | 8/4 | 38.62 | 67.17 | 64.57 | 72.47 | 56.28 | 41.31 | 71.69 | 80.62 | 82.08 | 83.87 |
| FQ-ViT | 4/8 | 27.84 | 71.17 | 43.93 | 78.48 | 64.42 | 74.70 | 79.19 | 81.17 | 81.43 | 82.69 |
| PTQ4ViT | 4/8 | 59.23 | 69.68 | 36.04 | 67.99 | 66.57 | 76.96 | 79.47 | 79.62 | 78.50 | 82.54 |
| APQ-ViT (Ours) | 4/8 | 59.42 | 72.30 | 61.81 | 72.63 | 66.71 | 77.14 | 79.55 | 80.56 | 81.94 | 83.42 |
| FQ-ViT | 6/6 | 0.38 | 4.26 | 2.65 | 0.10 | 58.66 | 45.51 | 64.63 | 66.50 | 52.09 | 0.10 |
| PTQ4ViT | 6/6 | 64.46 | 78.63 | 71.90 | 81.65 | 69.68 | 76.28 | 80.25 | 82.38 | 84.01 | 85.44 |
| APQ-ViT (Ours) | 6/6 | 69.55 | 79.10 | 72.89 | 82.21 | 70.49 | 77.76 | 80.42 | 82.67 | 84.18 | 85.60 |
| FQ-ViT | 8/8 | 45.99 | 78.68 | 58.87 | 82.76 | 70.92 | 78.44 | 81.12 | 82.38 | 82.38 | 85.74 |
| PTQ4ViT | 8/8 | 74.56 | 81.00 | 75.58 | 84.25 | 71.72 | 79.47 | 81.48 | 83.10 | 85.14 | 86.36 |
| APQ-ViT (Ours) | 8/8 | 74.79 | 81.25 | 75.64 | 84.26 | 72.02 | 79.78 | 81.72 | 83.16 | 85.16 | 86.40 |

4.1 Settings

PTQ scheme: We first build a post-training quantization baseline for experiments, where we follow the [47] to set the search range of weight and activation to $[0, 1.2]$ for image classification task and follow [8, 30] and set to $[0.5, 1.2]$ for detection task, and evenly divide to $n = 100$ intervals. The default search rounds of the alternative optimization is 3. We randomly select 32 images from the ImageNet dataset for classification tasks and only 1 image from COCO dataset for detection tasks. We empirically set $\gamma = 10$ as default. The bit-width of the quantized model is marked as W_wA_a standing for w -bit weight and a -bit activation. As for comparison methods, we follow the official settings using the released codes.

Vision Tasks and Network Architectures: To prove the versatility of our AFQ-ViT, we evaluate it on image classification and detection tasks. We adopt the most widely-used transformer-based networks for comparison, including ViT [9], DeiT [41] and Swin Transformer [29] for classification task on ImageNet [7] and three different scales of Swin Transformer for detection task on COCO dataset [27]. Note that we do not quantize the activation in the first convolution layer and the last classification layer. We also keep the Softmax, LayerNorm and GeLU functions as full-precision since they cause little computational overheads, but quantizing them will cause a severe accuracy drop.

4.2 Ablation Study

We conduct extensive ablation studies on each proposed method. As Table 1 shows, we evaluate our methods on ViT-S, ViT-B and DeiT-B vision transformer architectures. The baseline post-training quantization method suffers a severe accuracy loss, especially under 4-bit setting. While our methods retain the accuracy and the advantage becomes more obvious in lower bit-width. Applying the BBC can significantly improve the performance. For example, it

helps ViT-B to get 38.40% accuracy in W4A4 which is 7.71% higher than the traditional method. As for the MPQ, we compare it with the Logarithmic quantizer and Segmental quantizer and evaluate ViT-S, DeiT-S and DeiT-B. As shown in Table 2, MPQ quantizer outperforms other quantizers by a wide margin, especially in W4A4. DeiT-S equipped with MPQ is 21.96% higher than the Logarithmic quantizer and 21.24% higher than the Segmental quantizer. We conjecture that it is because in the lower bit-width condition, the quantizer spares fewer bits to represent the large magnitude, especially for Logarithmic and Segmental quantizers, the negative influence of damaging Matthew-effect becomes manifest. Besides, the phenomena are consistent in 6-/8-bit settings.

Moreover, jointly applying the proposed methods can further improve the performance, which demonstrates that the BBC optimization strategy in conjunction with MPQ can work orthogonally.

4.3 Comparison on Classification Task

We first conduct extensive experiments on ImageNet classification tasks. We choose different transformer-based architectures, including ViT, DeiT and Swin Transformer. The default patch size is 16×16 and the image resolution is 224×224 if not specifically mentioned (ViT-S/32 means the patch size is 32×32 , Swin-B/384 means the image resolution is 384×384).

We highlight that APQ-ViT is versatile and has prevailing improvements over different transformer variants, patch sizes, input resolutions and bit-widths. As Table 3 shows, our method shows an impressive advantage especially in lower bit-width (*i.e.*, W4A4). We observe that previous methods like FQ-ViT almost crash when quantizing the activations to lower than 8-bit, while our APQ-ViT improves the accuracy significantly by up to 5.17% on average compared to PTQ4ViT under W4A4. For some specific models, like ViT-B, our method even outstrips PTQ4ViT by 10.72%.

Table 4: Comparison of different post-training quantization methods on object detection task under various bit-widths.

| Method | #bit(W/A) | Mask RCNN Swin-T | | Mask RCNN Swin-S | | Cascade Mask RCNN Swin-T | | Cascade Mask RCNN Swin-S | | Cascade Mask RCNN Swin-B | |
|----------------|-----------|-------------------|--------------------|-------------------|--------------------|--------------------------|--------------------|--------------------------|--------------------|--------------------------|--------------------|
| | | AP ^{box} | AP ^{mask} | AP ^{box} | AP ^{mask} | AP ^{box} | AP ^{mask} | AP ^{box} | AP ^{mask} | AP ^{box} | AP ^{mask} |
| Full-precision | 32/32 | 46.0 | 41.6 | 48.5 | 43.3 | 50.4 | 43.7 | 51.9 | 45.0 | 51.9 | 45.0 |
| BasePTQ | 4/4 | 0.9 | 0.9 | 12.6 | 11.8 | 1.3 | 1.2 | 8.4 | 7.7 | 4.0 | 3.7 |
| PTQ4ViT | 4/4 | 6.9 | 7.0 | 26.7 | 26.6 | 14.7 | 13.5 | 0.5 | 0.5 | 10.6 | 9.3 |
| APQ-ViT (Ours) | 4/4 | 23.7 | 22.6 | 44.7 | 40.1 | 27.2 | 24.4 | 47.7 | 41.1 | 47.6 | 41.5 |
| BasePTQ | 8/4 | 2.2 | 2.1 | 23.2 | 21.4 | 3.2 | 3.0 | 16.3 | 14.6 | 7.6 | 6.6 |
| PTQ4ViT | 8/4 | 25.5 | 25.0 | 18.3 | 18.0 | 18.4 | 16.7 | 32.7 | 29.0 | 14.4 | 13.1 |
| APQ-ViT (Ours) | 8/4 | 33.7 | 31.6 | 46.6 | 41.8 | 36.6 | 32.2 | 49.6 | 43.4 | 49.2 | 43.0 |
| BasePTQ | 4/8 | 42.4 | 38.8 | 45.7 | 41.0 | 45.5 | 40.0 | 47.4 | 41.5 | 47.2 | 41.6 |
| PTQ4ViT | 4/8 | 0.7 | 0.8 | 23.4 | 22.2 | 25.3 | 22.7 | 38.5 | 33.8 | 20.0 | 28.4 |
| APQ-ViT (Ours) | 4/8 | 43.1 | 39.3 | 47.3 | 42.2 | 46.2 | 40.7 | 49.4 | 43.0 | 49.0 | 42.9 |
| BasePTQ | 6/6 | 40.1 | 36.8 | 46.7 | 41.8 | 46.3 | 40.7 | 48.9 | 42.7 | 46.3 | 40.7 |
| PTQ4ViT | 6/6 | 5.8 | 6.8 | 6.5 | 6.6 | 14.7 | 13.6 | 12.5 | 10.8 | 14.2 | 12.9 |
| APQ-ViT (Ours) | 6/6 | 45.4 | 41.2 | 47.9 | 42.9 | 48.6 | 42.5 | 50.5 | 43.9 | 50.1 | 43.7 |
| FQ-ViT | 8/8 | 45.3 | 41.2 | 48.2 | 42.6 | 49.7 | 43.3 | 51.7 | 44.2 | 51.1 | 44.3 |
| BasePTQ | 8/8 | 45.8 | 41.5 | 48.1 | 42.9 | 48.6 | 42.5 | 50.3 | 43.8 | 49.9 | 43.7 |
| PTQ4ViT | 8/8 | 28.0 | 27.1 | 1.5 | 1.4 | 40.3 | 35.6 | 20.8 | 18.7 | 2.0 | 1.9 |
| APQ-ViT (Ours) | 8/8 | 45.8 | 41.5 | 48.3 | 43.1 | 48.9 | 42.7 | 50.8 | 44.1 | 50.2 | 43.9 |

Moreover, under W6A6 and W8A4 settings, the average accuracy improvement of APQ-ViT compared with the previous method is 1.02% and 3.87%, respectively. Under the W4A8 setting, our method accomplishes high accuracy. The average improvement compared with FQ-ViT is 5.05%, and that with PTQ4ViT is 3.88%. It is noteworthy that our methods achieve almost loss-less accuracy under W8A8. For instance, the DeiT-B and Swin-B/384 models quantized by APQ-ViT have only 0.08% and 0.04% accuracy drop, within 0.10%. And the average accuracy loss of W8A8 compared with the full-precision model is only about 0.23%.

4.4 Comparison on Object Detection Task

To further evaluate the generalization capability of our methods, we extend it to object detection tasks using large-scale COCO datasets. We use the Mask RCNN and Cascade Mask RCNN detectors with Swin Transformers (Swin-T/S/B) as backbones.

The results are presented in Table 4. We highlight that compared to classification tasks, quantizing activation to lower-bit, *e.g.*, W4A4 and W8A4, usually brings more challenges to model robustness and accuracy of detection tasks. Models calibrated by previous methods almost crash, while APQ-ViT converges and recovers the accuracy. Especially under the W4A4 setting, the average improvement is a remarkable 24.43% and 30.81% over PTQ4ViT and BasePTQ respectively. For example, our APQ-ViT achieves 44.7% and 40.1% (drops 3.8% and 3.2%) for AP^{box} and AP^{mask} with Cascade Mask RCNN Swin-S, while PTQ4ViT methods only get 26.7% and 26.6%.

Furthermore, APQ-ViT with W6A6 and W4A8 settings also averagely outstrips the BasePTQ by 2.57% and 1.20%, respectively. As for W8A8, APQ-ViT gets comparable performance which only drops 0.18% and 1.20% compared to full-precision counterparts with

Mask RCNN detector and Cascade Mask RCNN detector. It shows great potential for low-bit quantized detectors to meet the accuracy requirements and be implemented in real-world applications.

In a nutshell, APQ-ViT is a versatile method that shows a great practical value on both image classification and object detection tasks over various bit-width and transformer variants.

5 CONCLUSION

In this paper, we analyze the post-training quantization for vision transformers from optimization and structure perspectives and propose a novel method, namely APQ-ViT. We first present a unified Bottom-elimination Blockwise Calibration scheme which fixes the overall quantization error in a blockwise manner and prioritizes the crucial errors that impact more on the final output. Moreover, we design a Matthew-effect Preserving Quantization to maintain the power-law distribution of Softmax and keep the function of the attention mechanism. Comprehensive experiments demonstrate that our APQ-ViT achieves prevailing improvements, especially in lower bit-width settings (*e.g.*, averagely up to 5.17% improvement for classification and 24.43% for detection on W4A4). We highlight that APQ-ViT is a versatile method that works well with diverse vision transformer variants, including DeiT and Swin Transformer.

ACKNOWLEDGEMENT

This work was supported by The National Key Research and Development Plan of China (2021ZD0110503), National Natural Science Foundation of China (62022009 and 61872021) and Meituan.

REFERENCES

- [1] Alham Fikri Aji and Kenneth Heafield. 2017. Sparse communication for distributed gradient descent. *arXiv preprint arXiv:1704.05021* (2017).
- [2] Haoli Bai, Lu Hou, Lifeng Shang, Xin Jiang, Irwin King, and Michael R Lyu. 2021. Towards efficient post-training quantization of pre-trained language models. *arXiv preprint arXiv:2109.15082* (2021).
- [3] Iz Beltagy, Matthew E. Peters, and Arman Cohan. 2020. Longformer: The Long-Document Transformer. *arXiv:2004.05150* (2020).
- [4] Nicolas Carion, Francisco Massa, Gabriel Synnaeve, Nicolas Usunier, Alexander Kirillov, and Sergey Zagoruyko. 2020. End-to-end object detection with transformers. In *European conference on computer vision*. Springer, 213–229.
- [5] Krzysztof Choromanski, Valerii Likhoshesterov, David Dohan, Xingyou Song, Andreea Gane, Tamas Sarlos, Peter Hawkins, Jared Davis, Afroz Mohiuddin, Lukasz Kaiser, et al. 2020. Rethinking attention with performers. *arXiv preprint arXiv:2009.14794* (2020).
- [6] Yoni Choukroun, Eli Kravchik, Fan Yang, and Pavel Kisilev. 2019. Low-bit quantization of neural networks for efficient inference. In *2019 IEEE/CVF International Conference on Computer Vision Workshop (ICCVW)*. IEEE, 3009–3018.
- [7] Jia Deng, Wei Dong, Richard Socher, Li Jia Li, Kai Li, and Fei Fei Li. 2009. ImageNet: a Large-Scale Hierarchical Image Database. In *IEEE CVPR*.
- [8] Wu Di, Tang Qi, Zhao Yongle, Zhang Ming, Zhang Debing, and Fu Ying. 2020. EasyQuant: Post-training Quantization via Scale Optimization.
- [9] Alexey Dosovitskiy, Lucas Beyer, Alexander Kolesnikov, Dirk Weissenborn, Xiuhua Zhai, Thomas Unterthiner, Mostafa Dehghani, Matthias Minderer, Georg Heigold, Sylvain Gelly, Jakob Uszkoreit, and Neil Houlsby. 2021. An Image is Worth 16x16 Words: Transformers for Image Recognition at Scale. *ICLR* (2021).
- [10] Patrick Esser, Robin Rombach, and Bjorn Ommer. 2021. Taming transformers for high-resolution image synthesis. In *Proceedings of the IEEE/CVF Conference on Computer Vision and Pattern Recognition*. 12873–12883.
- [11] Mark Everingham, Luc Van Gool, Christopher K. I. Williams, John Winn, and Andrew Zisserman. 2010. The Pascal Visual Object Classes Challenge. *IJCV* (2010).
- [12] Jun Fang, Ali Shafiee, Hamzah Abdel-Aziz, David Thorsley, Georgios Georgiadis, and Joseph H Hassou. 2020. Post-training piecewise linear quantization for deep neural networks. In *European Conference on Computer Vision*. Springer, 69–86.
- [13] Ross Girshick. 2015. Fast R-CNN. In *IEEE ICCV*.
- [14] Ross Girshick, Jeff Donahue, Trevor Darrell, and Jitendra Malik. 2014. Rich Feature Hierarchies for Accurate Object Detection and Semantic Segmentation. In *IEEE CVPR*.
- [15] Benjamin Graham, Alaeldin El-Nouby, Hugo Touvron, Pierre Stock, Armand Joulin, Hervé Jégou, and Matthijs Douze. 2021. LeViT: a Vision Transformer in ConvNet’s Clothing for Faster Inference. In *Proceedings of the IEEE/CVF International Conference on Computer Vision*. 12259–12269.
- [16] Haoyu He, Jing Liu, Zizheng Pan, Jianfei Cai, Jing Zhang, Dacheng Tao, and Bohan Zhuang. 2021. Pruning Self-attentions into Convolutional Layers in Single Path. *arXiv preprint arXiv:2111.11802* (2021).
- [17] Itay Hubara, Yury Nahshan, Yair Hanani, Ron Banner, and Daniel Soudry. 2021. Accurate post training quantization with small calibration sets. In *International Conference on Machine Learning*. PMLR, 4466–4475.
- [18] Kenneth E Iverson. 1962. A programming language. In *Proceedings of the May 1-3, 1962, spring joint computer conference*. 345–351.
- [19] Divyansh Jhunjhunwala, Advait Gadhihar, Gauri Joshi, and Yonina C Eldar. 2021. Adaptive quantization of model updates for communication-efficient federated learning. In *ICASSP 2021-2021 IEEE International Conference on Acoustics, Speech and Signal Processing (ICASSP)*. IEEE, 3110–3114.
- [20] Tianchu Ji, Shraddhan Jain, Michael Ferdman, Peter Milder, H. Andrew Schwartz, and Niranjana Balasubramanian. 2021. On the Distribution, Sparsity, and Inference-time Quantization of Attention Values in Transformers. In *Findings of the Association for Computational Linguistics: ACL-IJCNLP 2021*. Association for Computational Linguistics, Online, 4147–4157. <https://doi.org/10.18653/v1/2021.findings-acl.363>
- [21] Angelos Katharopoulos, Apoorv Vyas, Nikolaos Pappas, and François Fleuret. 2020. Transformers are rns: Fast autoregressive transformers with linear attention. In *International Conference on Machine Learning*. PMLR, 5156–5165.
- [22] Sehoon Kim, Amir Gholami, Zhewei Yao, Michael W Mahoney, and Kurt Keutzer. 2021. I-bert: Integer-only bert quantization. In *International conference on machine learning*. PMLR, 5506–5518.
- [23] Nikita Kitaev, Lukasz Kaiser, and Anselm Levskaya. 2020. Reformer: The efficient transformer. *arXiv preprint arXiv:2001.04451* (2020).
- [24] Krizhevsky, Alex, Sutskever, Ilya, Hinton, and E. Geoffrey. 2017. ImageNet Classification with Deep Convolutional Neural Networks. *Commun. ACM* (2017).
- [25] Manoj Kumar, Dirk Weissenborn, and Nal Kalchbrenner. 2021. Colorization transformer. *arXiv preprint arXiv:2102.04432* (2021).
- [26] Rundong Li, Yan Wang, Feng Liang, Hongwei Qin, Junjie Yan, and Rui Fan. 2019. Fully Quantized Network for Object Detection. In *IEEE CVPR*.
- [27] Tsung-Yi Lin, Michael Maire, Serge Belongie, James Hays, Pietro Perona, Deva Ramanan, Piotr Dollár, and C Lawrence Zitnick. 2014. Microsoft coco: Common objects in context. In *European conference on computer vision*. Springer, 740–755.
- [28] Yang Lin, Tianyu Zhang, Peiqin Sun, Zheng Li, and Shuchang Zhou. 2021. FQ-ViT: Fully Quantized Vision Transformer without Retraining. *arXiv preprint arXiv:2111.13824* (2021).
- [29] Ze Liu, Yutong Lin, Yue Cao, Han Hu, Yixuan Wei, Zheng Zhang, Stephen Lin, and Baining Guo. 2021. Swin Transformer: Hierarchical Vision Transformer using Shifted Windows. In *2021 IEEE/CVF International Conference on Computer Vision (ICCV)*. 9992–10002. <https://doi.org/10.1109/ICCV48922.2021.00986>
- [30] Zhenhua Liu, Yunhe Wang, Kai Han, Wei Zhang, Siwei Ma, and Wen Gao. 2021. Post-training quantization for vision transformer. *Advances in Neural Information Processing Systems* 34 (2021).
- [31] Sachin Mehta, Marjan Ghazvininejad, Srinivasan Iyer, Luke Zettlemoyer, and Hannaneh Hajishirzi. 2020. DeLight: Very Deep and Light-weight Transformer. arXiv:2008.00623 [cs.LG]
- [32] Sachin Mehta and Mohammad Rastegari. 2021. MobileViT: Light-weight, General-purpose, and Mobile-friendly Vision Transformer. *arXiv preprint arXiv:2110.02178* (2021).
- [33] Jiangmiao Pang, Kai Chen, Jianping Shi, Huajun Feng, Wanli Ouyang, and Dahua Lin. 2019. Libra R-CNN: Towards Balanced Learning for Object Detection. In *IEEE CVPR*.
- [34] Tim Prangemeier, Christoph Reich, and Heinz Koepl. 2020. Attention-based transformers for instance segmentation of cells in microstructures. In *2020 IEEE International Conference on Bioinformatics and Biomedicine (BIBM)*. IEEE, 700–707.
- [35] René Ranftl, Alexey Bochkovskiy, and Vladlen Koltun. 2021. Vision transformers for dense prediction. In *Proceedings of the IEEE/CVF International Conference on Computer Vision*. 12179–12188.
- [36] Shaoqing Ren, Kaiming He, Ross Girshick, and Jian Sun. 2016. Faster R-CNN: Towards Real-Time Object Detection with Region Proposal Networks. arXiv:1506.01497 [cs.CV]
- [37] Karen Simonyan and Andrew Zisserman. 2014. Very deep convolutional networks for large-scale image recognition. *arXiv preprint arXiv:1409.1556* (2014).
- [38] Xu Sun, Xuancheng Ren, Shuming Ma, and Houfeng Wang. 2017. meprop: Sparsified back propagation for accelerated deep learning with reduced overfitting. In *International Conference on Machine Learning*. PMLR, 3299–3308.
- [39] Christian Szegedy, Wei Liu, Yangqing Jia, Pierre Sermanet, Scott Reed, Dragomir Anguelov, Dumitru Erhan, Vincent Vanhoucke, and Andrew Rabinovich. 2015. Going Deeper With Convolutions. In *IEEE CVPR*.
- [40] Shitao Tang, Jiahui Zhang, Siyu Zhu, and Ping Tan. 2022. QuadTree Attention for Vision Transformers. *ICLR* (2022).
- [41] Hugo Touvron, Matthieu Cord, Matthijs Douze, Francisco Massa, Alexandre Sablayrolles, and Hervé Jégou. 2021. Training data-efficient image transformers & distillation through attention. In *International Conference on Machine Learning*. PMLR, 10347–10357.
- [42] Jiakai Wang, Aishan Liu, Zixin Yin, Shunchang Liu, Shiyu Tang, and Xianglong Liu. 2021. Dual Attention Suppression Attack: Generate Adversarial Camouflage in Physical World. arXiv:2103.01050 [cs.CV]
- [43] Yiru Wang, Weihao Gan, Wei Wu, and Junjie Yan. 2019. Dynamic Curriculum Learning for Imbalanced Data Classification. In *IEEE ICCV*.
- [44] Yiru Wang, Weihao Gan, Jie Yang, Wei Wu, and Junjie Yan. 2019. Dynamic Curriculum Learning for Imbalanced Data Classification. In *ICCV*.
- [45] Yanlu Wei, Renshuai Tao, Zhangjie Wu, Yuqing Ma, Libo Zhang, and Xianglong Liu. 2020. Occluded Prohibited Items Detection: An X-Ray Security Inspection Benchmark and De-Occlusion Attention Module. In *Proceedings of the 28th ACM International Conference on Multimedia*. 138–146.
- [46] Xucheng Ye, Pengcheng Dai, Junyu Luo, Xin Guo, Yingjie Qi, Jianlei Yang, and Yiran Chen. 2020. Accelerating CNN training by pruning activation gradients. In *European Conference on Computer Vision*. Springer, 322–338.
- [47] Zhihang Yuan, Chenhao Xue, Yiqi Chen, Qiang Wu, and Guangyu Sun. 2021. PTQ4ViT: Post-Training Quantization Framework for Vision Transformers. *arXiv preprint arXiv:2111.12293* (2021).
- [48] Manzil Zaheer, Guru Guruganesh, Kumar Avinava Dubey, Joshua Ainslie, Chris Alberti, Santiago Ontanon, Philip Pham, Anirudh Ravula, Qifan Wang, Li Yang, et al. 2020. Big bird: Transformers for longer sequences. *Advances in Neural Information Processing Systems* 33 (2020), 17283–17297.
- [49] Zhiyuan Zhang, Pengcheng Yang, Xuancheng Ren, Qi Su, and Xu Sun. 2020. Memorized sparse backpropagation. *Neurocomputing* 415 (2020), 397–407.
- [50] Mingjian Zhu, Kai Han, Yehui Tang, and Yunhe Wang. 2021. Visual transformer pruning. *arXiv e-prints* (2021), arXiv:2104.
- [51] Bohan Zhuang, Chunhua Shen, Mingkui Tan, Lingqiao Liu, and Ian Reid. 2019. Structured Binary Neural Networks for Accurate Image Classification and Semantic Segmentation. In *IEEE CVPR*.